Numerical study of a methanol spray flame

Shanglong Zhu[1,*], Dirk Roekaerts[2], Theo van der Meer[1]
[1] Laboratory of Thermal Engineering, University of Twente, the Netherlands
[2] Department of Multi-scale Physics, Delft University of Technology, the Netherlands

Abstract
In this study, the methanol spray flame in a chamber of the NIST was modelled, and the results were compared and validated by the experimental data. Features of this flame, including the boundary conditions of the inlet air and the spray, were analyzed according to the experiment for the numerical study. The standard k-ε model with the enhanced wall treatment was employed for the simulation of the turbulence. The predicted mean velocity components of the air flow at various downstream elevations showed good agreements with the experiment. For the spray and combustion, the Euler-Lagrange method and the steady flamelet model were employed. The droplet number density, SMD, and the mean axial and radial velocities of the droplets were compared to the measured data. In addition, the influence of the source term of the mixture fraction variance due to evaporation was investigated in this case. The results showed that including the source term, the peak mean mixture fraction variance, occurring in the lower part of the flame increased from 0.013 to 0.016 and the peak temperature increased by 10K.

1. Introduction

Liquid fuels are widely used in practical combustion systems such as industry boilers, internal combustion engines, and gas turbines. They usually are delivered into combustion chambers as turbulent sprays. The combustion efficiency, stability, and pollutant formation strongly depend on the characteristics of the turbulent spray combustion, and a better understanding of the turbulent spray combustion is required.

Experiments are usually considered as a desirable way for that, but it is difficult to measure combustion characteristics such as gas temperature and chemical species concentrations under many specific conditions. Numerical simulations have been attractive for many years because they provide an easy and safe way to understand the characteristics of combustion in detail. However, the modelling and simulation of the turbulent spray are particularly challenging because complex processes involving turbulence, atomization, evaporation, combustion and radiative heat transfer are included and they are strongly coupled. To improve the reliability of the spray combustion simulation, it is necessary to compare the prediction with experimental data and to test how the mathematical models perform.

To get a better understanding of the turbulent spray combustion system, often light oils were used. Their properties and detailed chemistry have been investigated repeatedly and are readily available. The reported experiment carried out by John F. Widmann and Cary Presser [1] at the National Institute of Standards and Technology (NIST) was conducted with methanol, and a database of methanol spray combustion was created. Several researchers [2,5,6] have used this database for the validation of their simulations. However, most of them focused on models only for some parts of the database and they seldom studied this case thoroughly taking the simulation of all the main processes into account.

In the present paper, the previous simulations are discussed and the features of this flame, including the boundary conditions of the inlet air and the spray, are analyzed to relate the experiment and simulations. We perform a numerical simulation in ANSYS Fluent with the steady flamelet model in order to include detailed chemistry and the influence of the evaporation on mixture fraction variance is investigated. Predictions of the mean velocity components of air flow and droplets, droplet number density, and Sauter Mean Diameter (SMD) are compared with the experimental data.

2. Experiment and previous simulations

The NIST flame experiment was carried out in a combustion chamber, shown in Fig.1. Swirling combustion air generated by a movable 12-vane swirl cascade passes through the outer annulus passage, with a flow rate $56.7 \pm 1.7\ \mathrm{m^3/h}$ and ambient pressure and temperature. A pressure-jet nozzle forms a hollow-cone methanol spray with a nominal 60° full cone angle at ambient temperature from the inner circular port. The nominal upstream pressure of the liquid fed to the nozzle is maintained at 690 kPa and the flow rate is maintained at 3.0 ± 0.02 kg/h.

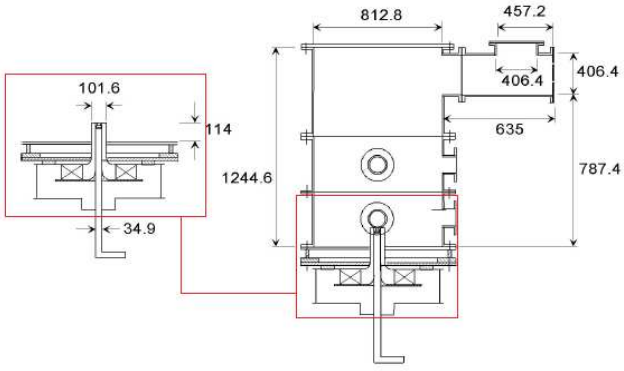

Fig.1. Setup and dimensions (mm) of the NIST flame experiment

Three gas velocity components at both cool and hot states were obtained from the PIV measurements

* Corresponding author: S.zhu@utwente.nl

at three downstream elevations within the chamber. Droplet size distributions, SMD, droplet mean axial and radial velocities, and droplet number density were measured at various axial locations downstream of the nozzle exit. Sheathed K-type thermocouples were used to measure the wall temperatures at various elevations and gas temperatures at the exit. Exit concentrations of CO_2, CH_3OH, CO were measured; no minor components or reaction intermediates was identified.

In previous simulations of the NIST flame, a simulation with Euler-Lagrange approach was done with 3D geometry by J. Collazo et al [2] also using Fluent. The interaction processes between droplets and continuous phase were simulated by use of Dispersed Phase model with the Linearized Instability Sheet Atomization (LISA) model of Schmidt et al. [3]. The standard k-ε model was used to simulate the turbulence. For combustion, the Eddy Dissipation Concept model proposed by Magnussen [4] was applied with a two-step reaction of methanol with oxygen and the decomposition of carbon dioxide. Predictions of droplet diameters, droplet trajectories, temperatures and gas concentrations are presented and compared with the NIST database [1]. The prediction of droplet properties showed some discrepancies, and the author deduced that the real spray angle should be higher than 60°. Temperatures and carbon dioxide at the exhaust of the system were well predicted in the simulation of [2], while the peak temperature of the flame was overestimated and the formation of unburned species was relatively inaccurate. Since the results of the velocities of both air and droplets were not presented, the turbulence model was not validated in this paper.

Also a mixture fraction based method has been used to simulate the NIST flame. De Jager [5] introduced a CFI model, in which C, F and I respectively represent a reaction progress variable, the mixing scalar and enthalpy scalar, to simulate the reacting spray combustion for this flame. The fluctuations are described by a β-PDF for c and f, and the δ-PDF for the enthalpy scalar i. The author indicated that turbulence is modelled poorly using the k-ε model, and the proposed spray model in its current form is limited and needs further improvement. The interaction between the spray and the combustion air needs more attention, especially in the near nozzle region. The influence of the spray on the gas phase turbulence is significant, but not seen in the model results. Suggestions were given from the author that it would be beneficial to implement spray effects in the model, to represent the effects of coalescence and secondary break-up, to reach a more accurate prediction of the SMD.

3. Mathematical models and boundary conditions

3.1. Grid and turbulence model

Convincing demonstration of grid independence is essential for reliable simulations and must be shown. However, grid independence in full 3D simulations is more difficult to be validated than in 2D simulations because of both complexity and computational cost, especially when there is a swirl and hybrid grids are employed.

For the simulation of the NIST flame, it was concluded through a 3-D CFD study of the experiment by Crocker et al. [6] that the influence of the exhaust channel on the simulation of the near-nozzle region was negligible and that it could be omitted in the geometry, considering the end of the combustion chamber as open boundary. As a result, the 2D axisymmetric swirl simulation is employed in the present study. It simplifies the 3D case into a 2D case with circular cylindrical coordinates.

The grid independence was then tested by introducing a series of different element sizes with the same aspect ratio of 3. The role of the near-wall treatment for this swirling flow was analyzed. As a result a 2D mesh with about 46000 quadrilateral cells (as shown in Fig.2) and the second order upwind scheme were found suitable for this study. A standard k-ε turbulence model with the enhanced wall treatment is employed based on the comparative analysis.

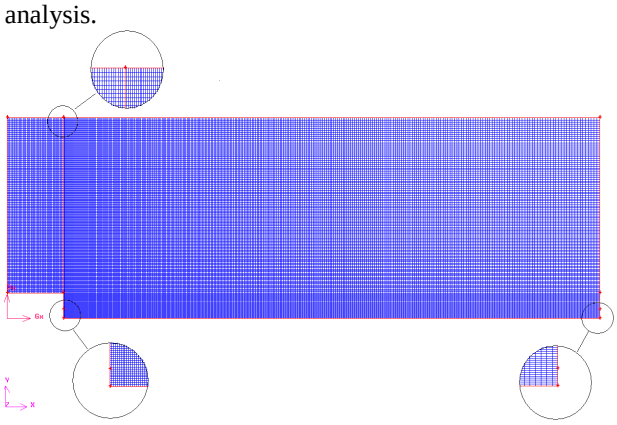

Fig.2. 2D mesh with about 46000 quadrilateral cells

3.2. Spray model

The atomization process of light oil sprays is commonly modelled using a wave growth or aerodynamic theory that predicts spray parameters such as the spray angle and the drop diameter. The surface wave instability model proposed by Reitz, the Kelvin-Helmholtz/Rayleigh-Taylor (KHRT) Instability model by Patterson and Reitz and the Taylor Analogy Breakup (TAB) model by O'Rourke and Amsden are widely used atomization models. However, the coupling with the nozzle effects and the primary atomization is largely unknown and is usually represented by an arbitrary nozzle-dependent constant.

For the pressure swirl atomizer in the NIST flame, we employ the LISA model. It assumes that Kelvin-Helmholtz waves grow on the sheet and eventually break the liquid into ligaments. It is then assumed that the ligaments break up into droplets due to varicose instability. Once the liquid droplets are

formed, the spray evolution is determined by drag, collision, coalescence, and secondary breakup.

For film formation, the relationship between the thickness of this film, t, and the mass flow rate is as follows:

$$\dot{m}_{eff} = \pi \rho u t (d_{inj} - t) \quad (1)$$

where d_{inj} is the injector exit diameter, $\dot{m}_{eff}$ is the effective mass flow rate, and u is the axial component of velocity at the injector exit. Because u depends on internal details of the injector and is difficult to calculate from first principles, the approach of Han et al. [7] is used and the total velocity is assumed to be related to the injector pressure by:

$$U = k_v \sqrt{\frac{2\Delta P}{\rho_l}} \quad (2)$$

where k_v is the velocity coefficient and a function of the injector design and injection pressure [8]. If ΔP is known, u can be calculated as

$$u = U \cos\theta \quad (3)$$

where θ is the spray angle.

For sheet breakup and atomization, the pressure-swirl atomizer model includes the effects of the surrounding gas, liquid viscosity and surface tension on the breakup of the liquid sheet. It is based upon the growth of sinuous waves on the liquid sheet. For waves that are long compared with the sheet thickness, ligaments are assumed to form from the sheet breakup process once the unstable waves reach critical amplitude. If the surface disturbance has reached a value of η_b at a breakup time τ, the sheet breaks up and ligaments will be formed at a length given by:

$$L_b = U_\tau = \frac{U}{\Omega} \ln\left(\frac{\eta_b}{\eta_O}\right) \quad (4)$$

where Ω is the maximum growth rate, and $\ln\left(\eta_b / \eta_O\right)$ is an empirical sheet constant. The default value of 12 was obtained theoretically by Weber [9] for liquid jets. Dombrowski and Hooper [10] showed that a value of 12 for the sheet constant agreed favourably with experimental sheet breakup lengths over a range of Weber numbers from 2 to 200.

Thus the diameter of the ligaments formed at the point of breakup can be obtained from a mass balance:

$$d_L = \sqrt{\frac{8h}{K_S}} \quad (5)$$

where K_S is the wave number corresponding to the maximum growth rate, and the film thickness can be calculated from the breakup length and the radial distance from the centre line to the mid-line of the sheet at the atomizer exit r_0:

$$h_{end} = \frac{r_0 h_0}{r_0 + L_b \sin\left(\frac{\theta}{2}\right)} \quad (6)$$

For waves that are short compared to the sheet thickness, the ligament diameter is assumed to be linearly proportional to the wavelength that breaks up the sheet:

$$d_L = \frac{2\pi C_L}{K_S} \quad (7)$$

where C_L is the ligament constant and equal to 0.5 by default.

In either the long-wave or the short-wave case, the breakup from ligaments to droplets is assumed to behave according to Weber's [9] analysis for capillary instability. So the most probable diameter for droplet diameter distribution, d_0, is determined from:

$$d_0 = 1.88 d_L \left(1 + 3Oh\right)^{1/6} \quad (8)$$

where Oh is the Ohnesorge number which is a combination of the Reynolds number and the Weber number.

Once this most probable droplet size of a Rosin-Rammler distribution has been determined, with a spread parameter of 3.5 and a default dispersion angle of 6° which are based on past modelling experience [11], the droplet diameter distribution is determined.

In the simulation, the fuel is assumed to be injected into the chamber as a fully atomized spray consisting of spherical droplets of various sizes. The motions of the droplets in the turbulent combustion flow field are calculated using a stochastic tracking method so that the momentum, mass, and energy exchange between the droplets and the gas phase can be simulated by tracking a large number of droplets.

The equation of motion for a droplet is represented as:

$$\frac{du_{p,i}}{dt} = \frac{18\mu}{\rho_p D_p^2} \frac{C_D \,\mathrm{Re}}{24} \left(U_i - u_{p,i}\right) + \frac{g_i \left(\rho_p - \rho\right)}{\rho_P} + F_i \quad (9)$$

In this equation, u_p is the particle velocity, U is a sampled gas velocity, μ is the molecular viscosity of the fluid, ρ_p is the fluid density, ρ is the density of the particle, D_P is the particle diameter, Re is the relative Reynolds number and the drag coefficient C_D is a function of the particle Reynolds number. F_i is an additional acceleration term.

As for secondary breakup, The Taylor analogy breakup (TAB) model, which is based upon Taylor's analogy [12] between an oscillating and distorting droplet and a spring mass system, is employed in the simulation of the NIST flame, since this case has low-Weber-number injections and the TAB model is

well suited for low-speed sprays into a standard atmosphere.

For droplet collision and coalescence, the algorithm of O'Rourke [13] is employed. It uses the concept of a collision volume to calculate the probability of collision. In general, once two parcels are supposed to collide, the outcome tends to be coalescence if the droplets collide head-on, and bouncing if the collision is more oblique. The probability of coalescence can be related to the offset of the collector droplet centre and the trajectory of the smaller droplet. The critical offset is a function of the collisional Weber number and the relative radii of the collector and the smaller droplet.

The rate of vaporization is governed by gradient diffusion, with the flux of droplet vapour into the gas phase related to the difference in vapor concentration at the droplet surface and the bulk gas:

$$N_i = k_c \left(C_{i,s} - C_{i,\infty} \right) \tag{10}$$

where N_i is the molar flux of vapour, k_c is the mass transfer coefficient, $C_{i,s}$ is the vapour concentration at the droplet surface, and $C_{i,\infty}$ is the vapour concentration in the bulk gas. The concentration of vapour at the droplet surface is evaluated by assuming that the partial pressure of vapour at the interface is equal to the saturated vapour pressure, p_{sat}, at the particle droplet temperature, T_p:

$$c_{i,s} = \frac{p_{sat}\left(T_p\right)}{RT_p} \tag{11}$$

where R is the universal gas constant.

3.3. Radiation and combustion model

According to the analysis of the NIST flame, radiative heat transfer can not be neglected in the simulation of the NIST flame. The Discrete Ordinates (DO) radiation model with a variable absorption coefficient, weighted-sum-of-gray-gases model (WSGGM), is employed.

As combustion model, one-step global reaction mechanisms with the Eddy Dissipation Model (ED) are generally used in spray combustion simulations. However, detailed chemistry is necessary for the prediction of ignition and extinction processes, as well as the pollutant formation. The Eddy Dissipation Concept (EDC) model with detailed chemistry widely used in gaseous combustion seems to be attractive. However, due to the strong coupling between the equations with considerable change of density for spray combustion, the calculation with this approach did not converge well.

The flamelet model provides a feasible way to include detailed chemical reactions in turbulent combustion simulations without a considerable increase in computational time. The flamelet structure depends on the mixture fraction, ξ, and on scalar dissipation rate, χ in gas phase combustion. The Favre-averaged values of quantities in the turbulent flame are then obtained through the use of Favre-averaged probability density function, $\tilde{f}(\xi,\chi)$:

$$\tilde{\Phi} = \int_0^\infty \int_0^1 \Phi(\xi,\chi)\,\tilde{f}(\xi,\chi) d\xi d\chi \tag{12}$$

The detailed reaction mechanism for methanol employed in the present study was developed by R.P. Lindstedt and M.P. Meyer at University of California at Berkeley. It comprises 32 species and 167 reactions.

Furthermore, in order to investigate the influence of a source term due to evaporation in the mixture fraction variance equation, $\bar{\rho}_s \tilde{\xi}''^2 (1-2\tilde{\xi})\tilde{\xi}$, see [14], calculations were made without and with this source terms included.

3.4. Boundary conditions

It's clear that an accurate representation of the boundary conditions is essential to carrying out a successful simulation [15]. With respect to the air inlet conditions, the mass flow and the temperature for the simulation are shown in Tab.1. The air velocity components at downstream elevation z=1.4mm near the air inlet both with and without the spray are measured in the experiment. Based on the previous simulations and analysis, the velocity components at this elevation can represent the inlet conditions, and the data measured when the spray is present are supposed to be a better assumption for the simulation of the spray combustion.

For the walls, a convection coefficient with the ambient of 12 $Wm^{-2}K^{-1}$ and a surrounding ambient temperature of 298 K also used in J.Collazo's work [2] are adopted.

With regard to the spray, the mass flow rate, temperature of methanol, the injector pressure and spray angle for the simulation based on the experiment are shown in Tab.1. However, the injector exit diameter, d_{inj}, in equation (1) and the parameters for the droplet diameter distribution in LISA model are not clear and we have to deduce them from the experimental data.

Tab.1. Inlet conditions of air and fuel

Air flow rate (m^3/h)	~ 56.7 [a]
Air temperature (K)	298
Fuel flow rate (kg/h)	3.0
Fuel temperature (K)	298
Injection pressure (Pa)	690000
Spray angle	60°

a: interpolated data within relative error of 5%

The droplet number density at seven axial locations downstream of the nozzle exit (z = 5, 15, 25, 35, 45, 55, and 65 mm) from the experiment [1] was analyzed to estimate the injector exit diameter, as shown in Fig.3.

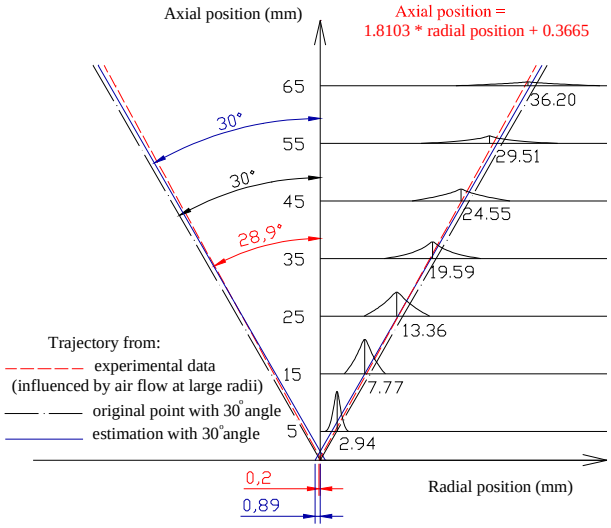

Fig.3. Estimation of the radial location of the spray

As a result, the injector exit diameter is estimated to be about 1.78 mm. Furthermore, the influence of the dispersion angle, sheet constant and ligament constant on the predicted results were investigated, and a combination of a dispersion angle of 10°, a sheet constant of 12 and a ligament constant of 0.5 was employed in our simulations.

4. Results and Discussion

Fig.4 shows the predicted mean velocity components at different downstream elevations compared with experiment. The bar at each point of the experimental data represents the uncertainty of the measurement.

It is clear that at large radii (＞17.45mm), where the air flow, instead of the spray, dominates the flow field, the results resemble the experimental data well. The deviations at large radii for the tangential velocity at z=9.5mm and z=17.6mm looks like considerable. However, if we take into account the influence of the considerable uncertainties of the data at z=1.4mm, which are considered as the inlet condition, the deviations are still minor. When it goes to the small radii, deviations against the experimental data for axial and radial velocities can be observed. This is also reported in other research [2,5]. One explanation is that the interaction between the droplets and the continuous phase is overestimated. However, because the acceleration of the continuous phase by the spray and thermal expansion of the continuous phase do result in the higher velocity components, an alternative more reasonable explanation is that it is difficult to measure velocity components of a gaseous phase in a region where a dispersed phase is present in high concentration. For the tangential velocity, the predicted results at small radii resemble the experimental data well because the tangential velocity is not accelerated by the spray.

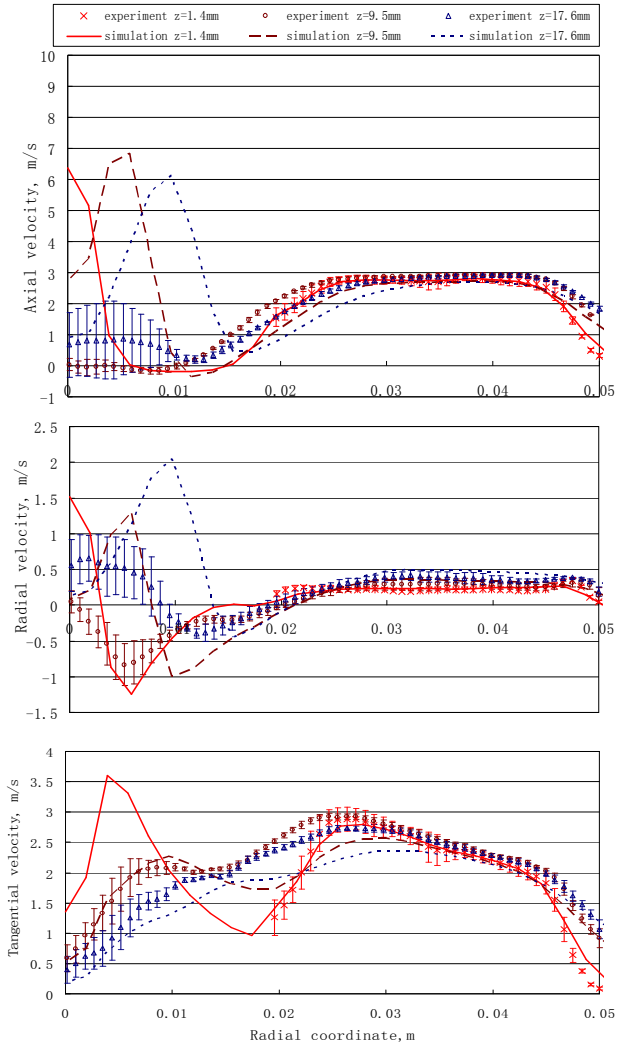

Fig.4. Predicted mean velocity components at different downstream elevations (z=1.4mm, 9.5mm and 17.6mm) compared with experiment

Fig.5. shows the predicted droplet number density at different downstream elevations compared with experiment. The peak points and trends are all in good agreement with the experimental data. The main difference here is that the simulation provides more droplets than the experiment, and the closer to the atomizer, the more overestimation it has. This is reasonable because accurate measurements of droplet number density in the high number density region close to the nozzle are very difficult, and that is why it is always suggested to be used in a qualitative way rather than quantitatively [1].

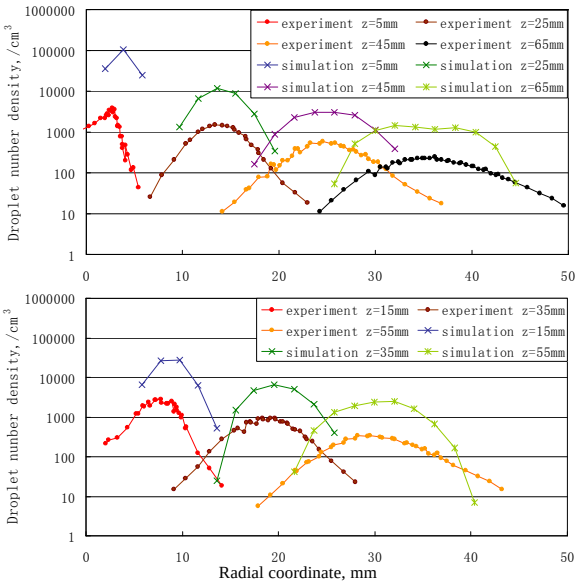

Fig.5. Predicted droplet number density at different downstream elevations compared with experiment

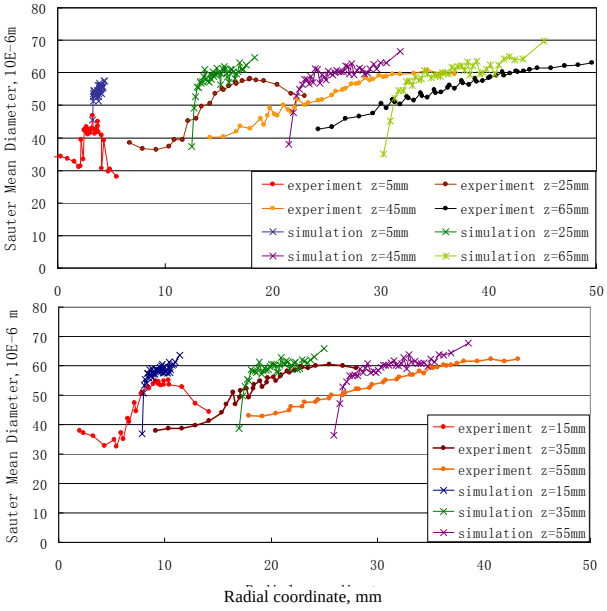

Fig.6. Predicted SMD of the droplets at different downstream elevations compared with experiment

Fig.6 shows the predicted SMD of the droplets. In consideration of the uncertainties of measurements and the calculation of SMD with the captured droplets, the predictions are pretty good. It seems that at z=5mm the SMD have higher deviations than at other elevations. That might be because at the nozzle exit the spray is directed inwards toward the symmetry axis. In a 2D simulation all droplets then travel via the axis and the coalescence is overestimated according to the algorithm of O'Rourke and causes the droplet diameters to be more narrowly distributed. It is to be noted that the simulation does not predict any SMD in the inner region of the cone because no droplets reach that region, in contrast with the experiment.

The predicted mean axial and radial velocities of the droplets are shown in Fig.7. They are in good agreements with the experiment also and have the same problem as the SMD predictions.

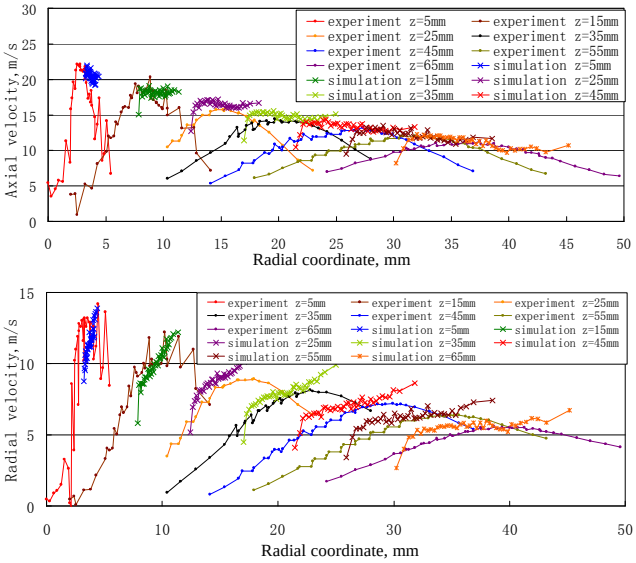

Fig.7. Predicted mean axial and radial velocities of the droplets at different downstream elevations compared with experiment

The contours of mean temperature are shown in Fig.8. The peak temperature is about 1850K, and the average temperature at the outlet here is about 700K. However, in the experiment they only measured a temperature of about 550K at the exit of the exhaust channel, which is omitted in the present study. Since this exhaust is further downstream as in the present computational domain, the temperature of 700 K is compatible with temperature at the exhaust of 550 K.

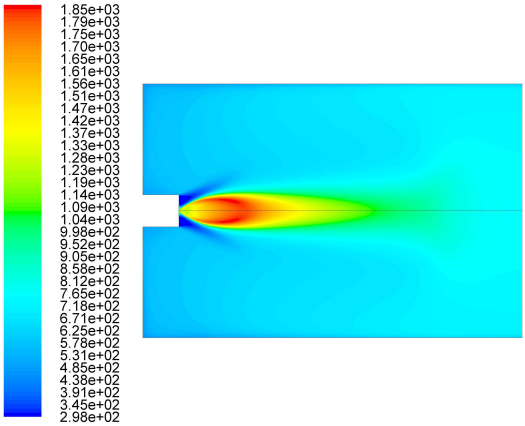

Fig.8. Contours of mean temperature [K]

As for the profile of the flame, here we introduce the definition of oxidation mixture ratio [16]

$$R_O = \frac{m_O}{m_O + \sum_c S_c m_{F,c}} \qquad (13)$$

where $s = n_O M_O / n_F M_F$ with m_O the mass fraction of oxygen, n the stoichiometric ratio, M is the molar mass, and index O, F, C representing oxygen, fuel and flue gas respectively. The lean flammability can be used to define the external boundary of the flame and the rich flammability can be used to define the inner boundary of the flame. We assume $R_O = 0.99$ is external boundary here [16], as shown in Fig.9. It resembles the flame profile in the experiment well and verifies that the mean concentration of OH in Fig.10 is related to the profile of the flame.

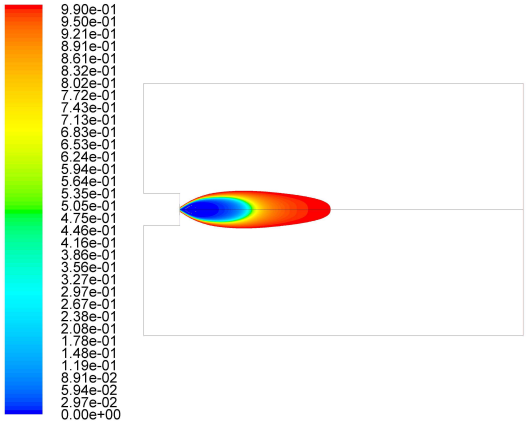

Fig.9. Contours of mean oxidation mixture ratio, R_O

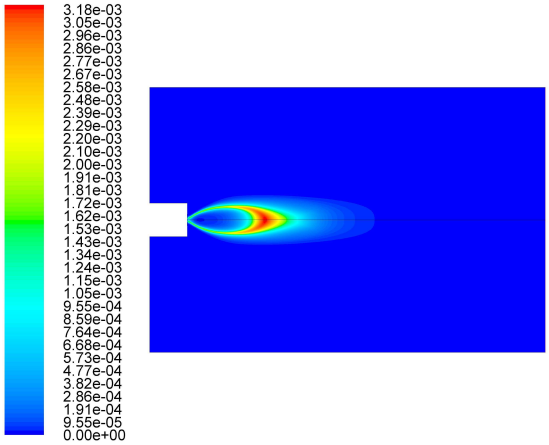

Fig.10. Contours of mean mole fraction of OH

The predicted contours of mean temperature with the source term of the mixture fraction variance because of evaporation taken into account are shown in Fig.11. The peak temperature is within 10K higher than without the evaporation source term and the high temperature region is a little contracted.

The mean mixture fraction variance with and without the source term are compared in Fig.12. Due to the evaporation of the droplets, the peak value of mean mixture fraction variance rises from 0.013 to 0.016, and the main difference occurs at the root of the flame, where most of the evaporation takes place. This is also the same region where the scalar dissipation changes with the peak value of scalar dissipation increasing from 13 s^{-1} to 17 s^{-1}. The obtained information about the injected droplets is also investigated and no considerable change is observed. Since in the NIST flame the influence of the source term on the mixture fraction variance only occurs in this lower region while the combustion mainly occurs in the flame area, the combustion characteristics are not strongly influenced by the modelling of the variance equation.

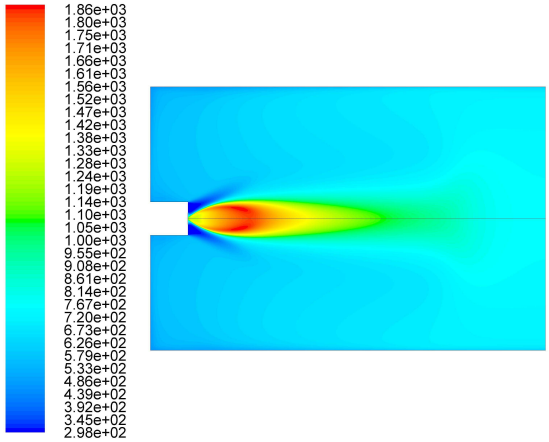

Fig.11. Contours of mean temperature with the influence of the evaporation on mixture fraction variance taken into account [K]

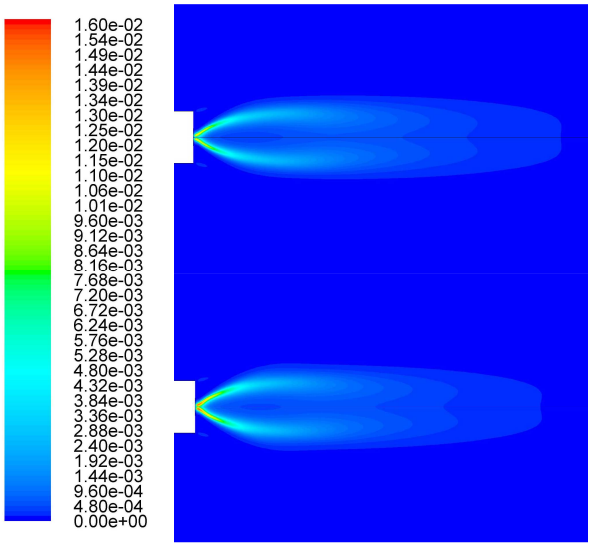

Fig.12. Comparison of mean mixture fraction variance (upper: without the source term due to evaporation, lower: with the source term)

5. Conclusions

In this study, the methanol spray flame in a chamber studied experimentally at the NIST was numerically investigated. The Euler-Lagrange method and the steady flamelet model with a detailed reaction mechanism of R.P. Lindstedt and M.P. Meyer were employed. In addition, the effect of the source term of the mixture fraction variance due to evaporation was also investigated numerically.

With the standard k-ε model and the enhanced wall treatment, the predicted mean velocity

components of the air flow at various downstream elevations showed good agreements with the experimental data. The deviations at small radii may be attributed to both numerical and experimental causes.

The droplet number density, SMD, and the mean axial and radial velocities of the droplets were validated by the measured data. It seems that in the simulation the droplets were more centralized distributed than in the experiment especially when it's close to the nozzle.

Due to the evaporation process, the peak value of mean mixture fraction variance increased from 0.013 to 0.016. However, the change only occurred in the lower part of the flame and not in the main flame area, so the combustion characteristics do not change much.

Acknowledgements

The authors would like to thank the Technology Foundation STW for financial support.

References

[1] John F. Widmann and Cary Presser, A benchmark experimental database for multiphase combustion model input and validation, Combust and Flame 129(2002)47–86.

[2] J. Collazo, J. Porteiro, D. Patiño, J.L. Miguez, E. Granada, J. Moran, Simulation and experimental validation of a methanol burner, Fuel 88 (2009) 326–334

[3] D. P. Schmidt, I. Nouar, P. K. Senecal, et al, Pressure-swirl atomization in the near field. SAE Paper 01-0496, SAE, 1999.

[4] Magnussen B.F. On the structure of turbulence and a generalized eddy dissipation concept for chemical reaction in turbulent flow. 19th AIAA Meeting, St. Louis, 1981.

[5] Bram de Jager, Combustion and noise phenomena in turbulent alkane flames, PhD thesis, Twente University, 2008.

[6] Crocker, D.S., Widmann, J.F., Presser, C., CFD modeling and comparison with data from the NIST reference spray combustor, ASME International Mechanical Engineering Congress and Exposition, 2001

[7] Z. Han, S. Perrish, P. V. Farrell, and R. D. Reitz. Modeling Atomization Processes of Pressure-Swirl Hollow-Cone Fuel Sprays. Atomization and Sprays, 7(6):663–684, 1997.

[8] A. H. Lefebvre. Atomization and Sprays. Hemisphere Publishing Corporation, 1989.

[9] C. Weber. Zum Zerfall eines Flüssigkeitsstrahles. ZAMM, 11:136–154, 1931.

[10] N. Dombrowski and P. C. Hooper. The effect of ambient density or drop formation in sprays. Chemical Engineering Science, 17:291–305, 1962.

[11] D. P. Schmidt, M. L. Corradini, and C. J. Rutland. A Two-Dimensional, Non-Equilibrium Model of Flashing Nozzle Flow. In 3rd ASME/JSME Joint Fluids Engineering Conference, 1999.

[12] G. I. Taylor. The Shape and Acceleration of a Drop in a High Speed Air Stream. Technical report, In the Scientific Papers of G. I. Taylor, ed., G. K. Batchelor, 1963.

[13] P. J. O'Rourke. Collective Drop Effects on Vaporizing Liquid Sprays. PhD thesis, Princeton University, Princeton, New Jersey, 1981.

[14] C.Hollmann and E.Gutheil, Modeling of turbulent spray diffusion flames including detailed chemistry, Twenty-sixth symposium (international) on combustion. The combustion institute, (1996)1731-1738.

[15] Cary Prresser, Application of a benchmark experimental database for multiphase combustion modeling, Journal of propulsion and power, Technical Note,22(2006)1145-1148.

[16] Ashwani K.Gupta, David G.Lilley, High temperature air combustion [M], Environmental and energy engineering Series, 2003, chapter1.2.2.2